

What is the flow activation volume of entangled polymer melts?

José A. Martins · Vera S. Cruz · Joanna Krakowiak · Weidong Zhang

Received: 3 August 2011 / Revised: 19 September 2011 / Accepted: 21 September 2011 / Published online: 4 October 2011
© Springer-Verlag 2011

Abstract We evaluate the flow activation volume in polymer melts of isotactic polypropylene and atactic polystyrene with step-shear experiments at different melt temperatures. The melt is initially sheared with constant shear rate until the attainment of a melt state with nearly constant viscosity. Perturbations to this experiment, involving shear steps in short-time intervals with decreasing rates, are induced next. Measurements of the shear stress value at each shear rate step allow the evaluation of an experimental (apparent) flow activation volume. The true flow activation volume is evaluated by extrapolating the experimental data to infinite shear stress values. The value obtained is larger than the physical volume of the chain and agrees with the volume of a tube confining chains with a molecular weight between M_n and M_w . Besides supporting the validity of tube model, experiments based on this protocol may be used on model polymer samples, in composites with nanoparticles and in polymer blends to access the validity of mechanisms considered by flow models.

Keywords Tube model · Flow activation volume · Step-shear · Viscosity

Introduction

It is not clear what units of polymer chains control the flow of melts at the high temperature Arrhenian flow region. Analysis of the segmental relaxation time obtained from NMR experiments with unentangled and entangled polymers, melts and solutions, concluded either that flow proceeds by conformational transitions only [1] or that these transitions are not the fundamental motions for flow [2]. These diverging conclusions were based on comparisons for the value of the parameter obtained by fitting the segmental relaxation time to a Vogel–Tamman–Fulcher or an Arrhenius equation with the flow activation energy (E_a) evaluated from rheological experiments. An agreement between the fitting parameter and E_a supported the first conclusion while a disagreement supported the latter.

The existing different versions of flow models have not contributed also to explain the issue. It is clear that the basic ideas of these models have experimental verification. Reducing the constraints of other chains to a test chain by confining it inside a tube with a diameter equal to the average distance between entanglements and a length equal to the average chain's length [3] and the movement of the test chain by reptation [4] were demonstrated with experimental results [5, 6]. However, formulations based only in these two concepts fail to explain the flow behaviour in the viscoelastic linear and nonlinear regimes. Different versions of these models evolved into complicated mathematical formulations, sometimes in disagreement with the experiments [7, 8]. For example, it is considered that because the tube consists of many other surrounding chains, the motion of the chains inside their tubes is independent of each other. It was demonstrated that cross-correlations between different chains, neglected in tube theory, are very significant and their role remains to be investigated [7, 8].

J. A. Martins · V. S. Cruz · J. Krakowiak · W. Zhang
Departamento de Engenharia de Polímeros,
Universidade do Minho,
Campus de Azurém,
4800-058, Guimarães, Portugal

J. A. Martins (✉) · V. S. Cruz · J. Krakowiak · W. Zhang
CICECO, Universidade de Aveiro,
3810-193, Aveiro, Portugal
e-mail: jamartins@dep.uminho.pt

We present in this work a new experimental protocol to evaluate the flow activation volume in polymer melts. The protocol was inspired by the transient experiments used to evaluate the flow activation volume in the plastic deformation of metals [9]. The theory behind this evaluation is the rate theory of plastic deformation. The values evaluated for the flow activation volume elucidated the deformation mechanisms in metals and received experimental confirmation by in situ observations of dislocations moving in a sample strained in a transmission electron microscope or in a synchrotron beam [10].

Flow activation volumes evaluated for deformation processes of solid polymers are around 10 nm^3 and involve the movement of ~ 200 carbon atoms of the main chain [11, 12]. We expect larger flow activation volumes in the deformation of polymer melts. To identify the relevant volumes, we start by defining the physical volume of a chain with molecular weight M and the volume of a tube confining that chain. We present afterwards the basic equations of the rate theory of plastic deformation and show how to evaluate the flow activation volume from transient experiments, similar to the experiments used in the evaluations of flow activation volume in the plastic deformation of metals [9, 10] or in solid deformations of polymers [12].

In the tube model, the tube diameter a is also the average distance between two consecutive constraints of the chain. It is related to the number of statistical chain segments between entanglements ($n_{k,e}$), each one having a length equal to one Kuhn monomer (l_k), by

$$\langle a^2 \rangle = n_{k,e} \cdot l_k^2. \quad (1)$$

The number of tube sections in a chain with molecular weight M is $Z = M/M_e = M/n_{k,e}M_k$, where M_e is the molecular weight between entanglements and M_k is the molecular weight of a Kuhn monomer.

The volume of a tube confining this chain is

$$V_t = \pi \frac{a^3}{4} Z = \frac{\pi}{4} \frac{M_e^{1/2}}{M_k^{3/2}} \cdot l_k^3 \cdot M, \quad (2)$$

which may also be expressed in terms of the packing length (p) [13] or in terms of the number of chains within the confinement volume of a tube section between entanglements (P_e) [14] as

$$V_t = P_e v_e Z \quad (3)$$

with

$$P_e = \frac{\pi a^3}{4v_e} = \frac{\pi a^3}{4v_k n_{k,e}}, \quad (4)$$

where v_k the volume of a Kuhn monomer and v_e is the volume of a chain segment between entanglements. A

simpler definition of P_e is $P_e = V_{\text{tube}}/V_{\text{chain}}$, where V_{chain} is the physical volume of the chain.

The packing length [13] is defined as

$$p = \frac{V_{\text{chain}}}{\langle r^2 \rangle_0} = \frac{Z v_e}{\langle r^2 \rangle_0} = \frac{Z v_e}{Z n_{k,e} l_k^2} = \frac{v_e}{\langle r^2 \rangle_{0,e}} = \frac{v_k}{l_k^2} \quad (5)$$

where in the last equalities use was made of self-similarity property of Gaussian chains. Since $V_{\text{chain}} = n_k v_k$ and the volume of one Kuhn monomer is $v_k = \pi l_k h_k^2/4$, i.e., it may be viewed as a cylinder of length l_k and diameter h_k , the packing length may be expressed also as

$$p = \pi h_k^2/4l_k, \quad (6)$$

which may be used to evaluate the diameter of one Kuhn monomer from the packing length. This last equation is a direct result of the packing length definition in Eq. 5. The chain may then be viewed as made up of freely joined rods of length l_k and diameter h_k , with volume $V_{\text{chain}} = p \langle r^2 \rangle_0$, and the packing length is proportional to the ratio of the cross-sectional area to the length of each rod.

Substitution of Eq. 5 into Eq. 3 yields

$$V_t = P_e p Z \langle r^2 \rangle_{0,e} = P_e p \langle r^2 \rangle_0 = 6P_e p R_g^2, \quad (7)$$

which is an alternative formulation for the volume of a tube confining a chain with a specific average square end-to-end distance. The last equality is strictly valid for linear chains only. Since the quantities generally available to characterize the “size” of polymer chains are their different molecular weight averages, we will use Eq. 2 to evaluate the volume of a tube confining a chain with a specific molecular weight.

To evaluate the flow activation volume, the Eyring’s rate theory of plastic deformation is applied [9]. If the free energy barrier for dislocation of flow segments in the flow direction in absence of stress is ΔG_o , then the strain rate resulting from a shear stress τ is

$$\dot{\gamma}(\tau, T) = \dot{\gamma}_0 \exp \left[- \left(\Delta G_o - \tau V^* \right) / k_B T \right], \quad (8)$$

where $\dot{\gamma}_0$ is a constant, k_B the Boltzmann constant and T the absolute temperature. If both forward and backward transitions over the energy barrier are considered, Eq. 8 may be written in the more general form as

$$\dot{\gamma}(\tau, T) = 2A \sinh \left[\tau V^* / k_B T \right], \quad (9)$$

where $A = \dot{\gamma}_0 \exp[-\Delta G_o/k_B T]$.

The experimental evaluation of flow activation volume requires transient experiments or short-time perturbations of a monotonic test. These experiments are performed at different temperatures and the material’s response at each temperature to the small perturbations is recorded. A key

assumption of the theory is that the material's flow mechanism is not affected by the perturbations, or expressed in different words, the volume of the flow unit activated by flow remains unchanged by the perturbations.

The monotonic test selected for testing polymer melts was a deformation with constant shear rate. After the attainment of a melt state with nearly constant viscosity at the shear rate $\dot{\gamma}_1$, this test is perturbed by decreasing the shear rate to $\dot{\gamma}_2$. This last shear rate is applied during a short-time interval, short enough for ensuring the non-perturbation of the flow mechanism. The material responds to each shear rate step with a shear stress and the experimental flow activation volume V_e is evaluated as

$$V_e = k_B T \left[\frac{\ln(\dot{\gamma}_2 / \dot{\gamma}_1)}{\tau_2 - \tau_1} \right]_{T, \text{DefMech}} \quad (10)$$

Other equation yielding similar results as Eq. 10 may be derived directly from Eq. 8 as

$$V_e = k_B T \left[\frac{d \ln(\dot{\gamma})}{d \tau} \right]_{T, \text{DefMech}} \quad (11)$$

Experimental—apparent—(V_e) and true (V^*) FAV are different. As shown by Alefeld [15], a relationship between them may be obtained by inserting Eq. 9 into 11. The result is

$$V_e = \left(V^* + \tau \frac{\partial V^*}{\partial \tau} \right) \coth(\tau V^* / k_B T) \quad (12)$$

For very large values of τ , it is assumed that $\partial V^* / \partial \tau = 0$ and Eq. 15 may be written as

$$\frac{V_e}{k_B T} = \frac{V^*}{k_B T} \coth(\tau V^* / k_B T) = \alpha \coth(\alpha), \quad (13)$$

where α is the fitting parameter. For large stress values $V_e \approx V^*$. This equation has only one fitting parameter (α) that allows the true flow activation volume to be evaluated.

Experimental

The materials tested in this work were an atactic polystyrene (aPS) melt ($M_n=97,619$ g/mol, $M_w=205,000$ g/mol and $M_z=298,000$ g/mol with $M_e=14,800$ g/mol) and an isotactic polypropylene ($M_n=24,388$ g/mol, $M_w=150,596$ g/mol, $M_z=488,609$ g/mol with $M_e=5,500$ g/mol). The rheological experiments for evaluating the flow activation volume were performed in a Paar Physica rheometer with two different configurations: (a) parallel plates of 25 mm diameter at 220 °C and gap size of 0.7 mm and (b) cone-and-plate, with a cone angle of 2° and plate diameter of 25 mm. Experiments with gaps of 0.5 and 1 mm were also performed, yielding similar final results. To verify the results obtained, some

experiments were also repeated in an ARG2 rheometer from TA instruments. A set of reference experiments was performed with nitrogen atmosphere. Samples for these experiments were prepared from pellets melted at 200 °C and injected into a mould with a Thermo Scientific Mini Jet II injector. The mould temperature was set to 100 °C and an injection pressure of 400 bar was applied for 13 s. A second pressure of 200 bar was applied for 4 s.

The first step in the step-shear experiments consisted of a deformation with constant shear rate during a time long enough to stabilize the melt viscosity. Figure 1 shows results of this first step for different shear rates [16]. In the start-up of shear experiments, such as those of Fig. 1, the melt viscosity (or shear stress) increases initially, passes by a maximum at low strain values and decreases and stabilizes at a constant value. Using the language of the rate theory of plastic deformation, this first step is the monotonic test. In the step-shear experiments, this monotonic test is perturbed. This perturbation and its results are described in the next section.

Results and discussion

We start this section presenting details of the experimental protocol used in the step-shear experiments. The validity of results is discussed comparing the results obtained with different instruments at the same rate, melt temperature, different configurations and different shear steps. The evaluation of flow activation volume is presented next together with the fitting of data to the rate theory of plastic deformation. The true flow activation volume is evaluated and compared with physically meaningful volumes of polymer chains.

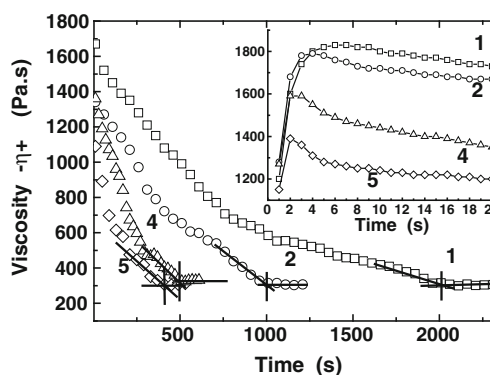


Fig. 1 Results of stress growth in shear for isotactic polypropylene. Transient viscosity measured at 220 °C with the parallel plate configuration at the shear rates indicated. The solid lines are graphical constructions to show the onset of the melt state with constant viscosity (indicated by the vertical lines). The inset shows the behaviour recorded for short shearing times indicating the maximum of viscosity at around 6 s.u.. Reprinted with permission from ref. [16]. Copyright 2006 American Chemical Society

The step-shear experiments

Figure 2 illustrates possible variations of the step-shear experiments for isotactic polypropylene. These results were obtained with different instruments using different configurations. Figure 2a, b shows the results obtained for the

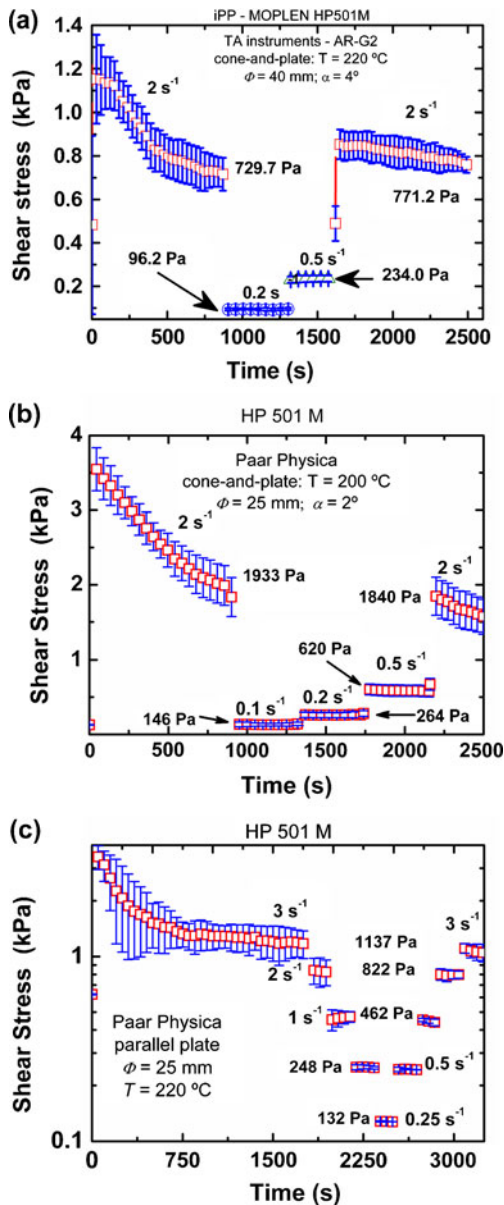


Fig. 2 Step-shear experiments with isotactic polystyrene at two different temperatures, with two different configurations, cone-and-plate and parallel plate, recorded in two different instruments. Results indicated are the average of five different experiments. The error bars are indicated. The first shearing step in the cone-and-plate configuration (a) and (b) was 900 s and that used for the parallel plate configuration in (c) was 1,800 s. This step was followed by shear steps at lower shear rates and shorter-time duration—400 s in (a) and (b) and 180 s in (c). In c, the variation of shear stress in two different steps at the same shear rate is around 5%. Average values of shear rate and shear stress in each step are indicated

cone-and-plate configuration with an AR-G2 and a Paar-Physica rheometer. The first step of these experiments was a controlled shearing with 2 s⁻¹ for 800 s. After this time, the monotonic test at 2 s⁻¹ was perturbed with shearing steps of lower shear rates and shorter-time duration. The final step was performed with a shear rate equal to that of the first step. The purpose of this last step was confirming that the shear stress value, and therefore the melt viscosity, returned at the end of the perturbation to the value of the first step and that the flow mechanism was not perturbed by the shear steps. We provide below further experimental confirmation of this assumption. This procedure allows also to ascertain if thermal degradation of the melt has affected, or not, the experimental results obtained. If this was the case, different shear stress values should have been obtained at the different shear steps.

The similarity of shear stress values for different steps with the same rate is clear in the experiment in Fig. 2c obtained with the parallel plate configuration. Here, the time duration of the first step was 1,800 s, more than the time required to establish a melt state with constant viscosity at the shear rate of 3 s⁻¹, around 750 s (see Fig. 1). This step was extended in time to guarantee the attainment of a state with nearly constant viscosity, as can be seen in Fig. 2c looking at the time interval between 750 s and 1,800 s.

Differences in the time duration of the first step for experiments performed with the parallel plate and cone-and-plate configurations are explained by the differences between the nominal shear rate and its average value in these two configurations. In the cone-and-plate configuration the shear rate is constant along the plate radius while in the parallel-plate configuration its average value is 2/3 the shear rate value at the edge of the plate. Therefore, the shearing time required to establish a melt state with nearly constant viscosity in the cone-and-plate configuration is $\sim 2/3$ that used for the parallel-plate configuration.

Results similar to those in Fig. 2 for isotactic polypropylene (iPP) were also obtained for an atactic polystyrene (see Fig. 3a). In this case, and based on results similar to those in Fig. 1 [16], the time duration of the first step at 230 °C for a shear rate of 4 s⁻¹ was set to 700 s. Similarly to the results in Fig. 2, this monotonic test was perturbed by shear steps with lower shear rates and shorter time duration. Stress values of the two final steps are different from those of the initial steps obtained with the same shear rate. For this reason, they were neglected in the flow activation volume evaluations. The different results of the two final steps may be ascribed to the sample thermal degradation.

Additional confirmation that the flow mechanism of the monotonic test was not unperturbed by the shear steps is provided in Fig. 3b. The average sample viscosity at the first step is depicted by the horizontal black dashed line and

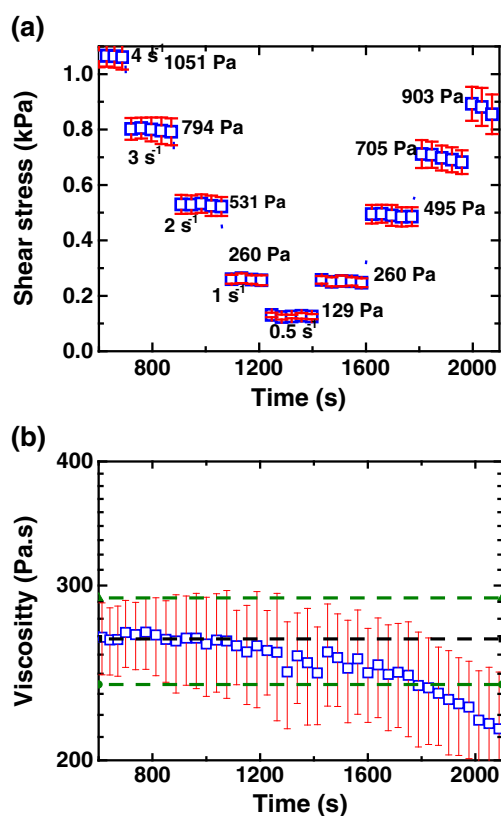


Fig. 3 **a** Step-shear experiments with atactic polystyrene melt at 230 °C recorded in a Paar Physica rheometer with the parallel plate configuration. The time duration of the first step at 4 s⁻¹ was 700 s and that of the remaining steps was 200 s. Symbols are average results of five experiments. The shear rate and the average values of shear stress for each step are indicated. **b** Melt viscosity variation during the perturbation experiment. Squares indicate the average result of five different experiments and error bars indicate the error is around the mean value. Black dashed line is the average viscosity value of the first step after viscosity stabilization. Dashed green lines are the accepted experimental error of viscosity measurements (10%)

its variation during the shear steps is indicated by open squares. The upper and lower horizontal dashed lines represent the accepted error in viscosity measurements, $\pm 10\%$ of the average value at the first step. Results for the last two steps are outside these lines and, as mentioned above, they were excluded from the flow activation volume evaluations. Other results are within these limiting two lines. They provide an additional indication that the flow mechanism was not perturbed by the shear steps.

Further confirmation that the results of the step-shear experiments were not affected by the instrument type or rheometer configuration is provided in Fig. 4a, b for iPP and aPS, respectively. They represent the experimental data according to Eq. 11. For the same melt temperature, they show that the stress variation at each shear step is the same, regardless the instrument or the configuration type used. The slope of these curves is the apparent flow activation volume. It increases with the shear stress and stabilizes at a

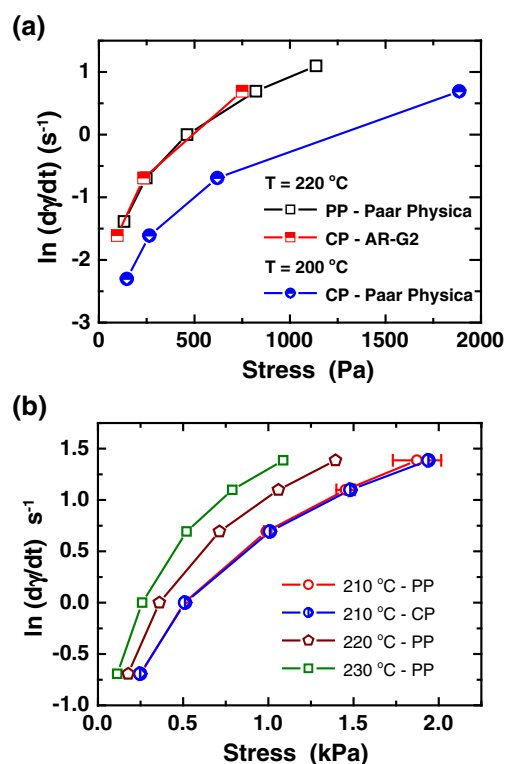


Fig. 4 Variation of the logarithm of the shear rate as function of the shear stress for polypropylene (**a**) and polystyrene (**b**) at the temperatures and with the configurations indicated. Values of shear stress and shear rate in these two figures are those in Figs. 2 and 3 with the exception of values at 220 and 230 °C for aPS whose experimental step-shear results are not shown here

constant value for large shear stress and lower temperature. The value evaluated under these conditions is the *true flow activation volume*.

True flow activation volume evaluation

Figure 5a shows the experimental flow activation volume of iPP evaluated with Eq. 10 using a procedure similar to that used in refs. [10] and [12]. The alternative evaluation with Eq. 11 is depicted in Fig. 5b. The results at the ordinate are the derivative of curves shown in Fig. 4a (circles) divided by $k_B T$, with $T=220$ °C. These two figures represent the two different procedures used to evaluate the flow activation volume. However, only the procedure used to construct Fig. 5b, based on Eq. 11, can be checked against a theory. Horizontal lines in both figures show the relevant volumes of polymer chains. Volumes indicated in Fig. 5a are the volume of a tube confining a chain with molecular mass M_w and the physical volume of a chain with M_w . For these evaluations, the following data were considered in addition: packing length value of iPP, $p=3.12$ Å [13], length and molecular weight of the Kuhn monomer, 11 Å and 180 g/mol, respectively [17]. The ratio $P_e = V_{\text{tube}}/V_{\text{chain}}$ of iPP is the

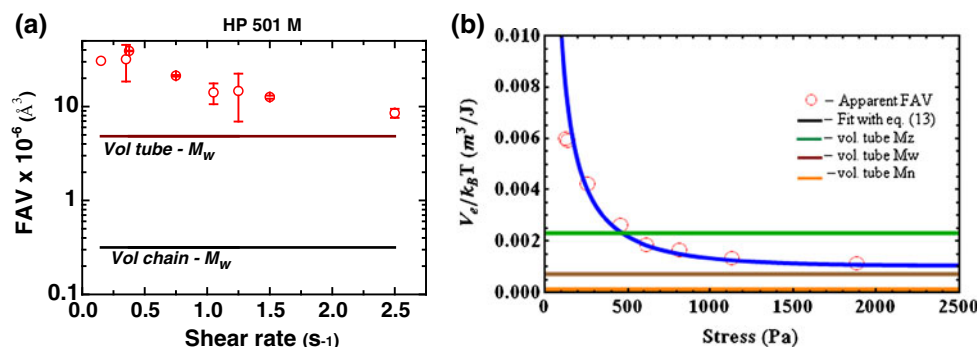


Fig. 5 Flow activation volume of isotactic polypropylene melt at 220 °C evaluated from the experimental data of Fig. 4a according to Eq. 10 in (a) and Eq. 13 in (b). The fit of the apparent flow activation volumes with Eq. 13 is indicated in (b) with a solid blue line. Horizontal solid lines indicate the volume of a tube confining a chain

number of chains within the volume confined by the tube. Its value, for the present case, is $P_e=15.3$. This concept was originally defined as the number of chains within the confinement volume of a tube section between entanglements [14], but due to the self-similarity property of Gaussian chains, it can be defined also as the number of chains within the volume confined by the tube.

The true flow activation volume obtained by fitting Eq. 13 to the experimental data in Fig. 5b is $6.87 \times 10^6 \text{ Å}^3$. It is around 40% above the volume of a tube confining a chain with M_w and one order of magnitude above the physical volume of the chain. Although these results were obtained for a highly polydisperse polymer ($M_w/M_n=6.2$), they do provide a clear indication that the true flow activation volume is much higher than the physical volume of the chain. It compares, in order of magnitude, to the volume of a tube confining the chain.

Similar results were also obtained for a different polymer, in this case, an atactic polystyrene of lower polydispersity, ≈ 2.1 . The results in Fig. 6 are the derivative of data shown in Fig. 4b. Their fit with Eq. 13 is indicated by the solid black line. The horizontal lines are the volumes of the tube confining the chains with M_w , M_n and the physical volume of a chain with M_w ($3.67 \times 10^5 \text{ Å}^3$). The dashed line shows the true flow activation volume, in this case $2.81 \times 10^6 \text{ Å}^3$. The volume of a tube confining the chain with M_w and the physical volume of the chain are $6.04 \times 10^6 \text{ Å}^3$ and $3.67 \times 10^5 \text{ Å}^3$, respectively. For these evaluations, we considered $p=3.92 \text{ Å}$, $l_k=18 \text{ Å}$ and $M_k=710 \text{ g/mol}$ [13, 17]. Also, in this case, it is clear that true flow activation volume is higher than the physical volume of the chain. The ratios $V^*/V_{\text{chain},M_w}=7.67$ and $V^*/V_{\text{chain},M_n}=16.11$ demonstrate clearly that true flow activation volume is the volume of a tube confining the chain motion. However, this volume cannot be precisely assigned to a chain with a specific molecular weight

with M_w and the physical volume of a chain with the same molecular weight in (a) and the volume of a tube confining the chains with M_z , M_w and M_n in (b). The volume of a tube confining a chain with M_w is $4.83 \times 10^6 \text{ Å}^3$ and the limiting value obtained for V^* is $6.97 \times 10^6 \text{ Å}^3$

For both polymers studied in this work, the true flow activation volume is much larger than the physical volume of the chain. The limiting value evaluated at an infinite shear stress (*true flow activation volume*) is between the volume of a tube confining the chains with M_n and M_w . We assign the lack of precision in the assignment of the true flow activation volume to polydisperse samples used in this work. Further experiments with model polymer samples of lower polydispersity could provide additional information on this aspect of the flow of polymer melts. It is our understanding that this information may help to clarify the validity of mechanisms considered by flow models. Our results support the validity of the tube model although they do not provide indication, or suggestion, of flow mechanisms in the viscoelastic linear regime.

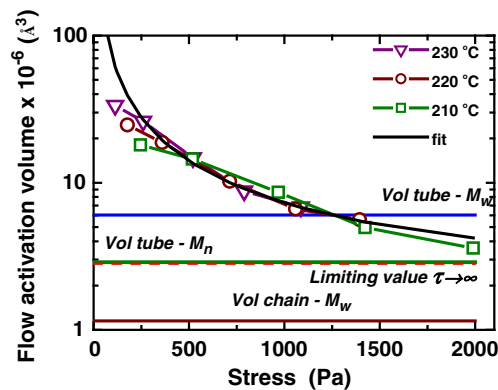


Fig. 6 The derivative of curves in Fig. 3 multiplied by $k_B T$, yielding the experimental flow activation volume of aPS. The true flow activation volume was obtained fitting the experimental data with Eq. 13. The only fitting parameter of this equation is equal to $4.05 \times 10^{-4} \text{ m}^3/\text{J}$, yielding a true flow activation volume for an infinite shear stress value of $2.81 \times 10^6 \text{ Å}^3$ (horizontal red dashed line) comparable to the volume of a tube confining the chains with M_n (horizontal green line). Horizontal lines indicate also the volume of a tube confining the chains with M_w and the physical volume of a chain with the same molecular weight

Because the volume of one Kuhn monomer for both polymers is around 10^3 \AA^3 , these results demonstrate also that flow in melts does not proceed by local and correlated conformational transitions. Although localized relaxations, involving the Kuhn monomer, the chain segments between entanglements and the Rouse relaxation of the chain, contribute to the chain's longest relaxation time and flow, the volume that activates the flow is that of tube confining the chain. Extension of these experiments to polymer solutions of different concentration, to entangled and unentangled polymer melts with lower polydispersity, and to polymer blends may provide additional information on the validity of flow mechanisms considered by theoretical models.

Conclusions

We presented a new protocol for rheological experiments. It consists of step-shear experiments performed at a melt state with nearly constant viscosity. The shear steps are perturbations induced to a monotonic test performed with constant shear rate at constant temperature. It was assumed that the flow mechanism was not affected by these perturbations. The validity of this assumption was demonstrated with experimental results.

The rate theory of plastic deformation was applied to the experimental results of step-shear experiments allowing the true flow activation volume to be evaluated. It was shown that this volume compares to the volume of a tube confining the chain. It is around one order of magnitude higher than the physical volume of the chain. Besides confirming the validity of tube model, these results suggest that their application to other polymer systems could help to clarify the validity of flow mechanisms considered by these models. Further relevant information may also be obtained

by applying this method to model polymer systems of lower polydispersity.

Acknowledgments We thank Andrzej Galeski for pointing us ref. [10]. We acknowledge the Portuguese Foundation of Science and Technology for funding the project FCOMP-01-0124-FEDER-007151 (PTDC/CTM/68614/2006). This work was supported by the European Community fund FEDER and project 3599/PPCDT.

References

1. Moe NE, Qiu X, Ediger MD (2000) *Macromolecules* 33:2145–2152
2. Qiu X, Ediger MD (2000) *Macromolecules* 33:490–498
3. Doi M, Edwards SF (1986) *The theory of polymer dynamics*. Oxford University Press, New York
4. de Gennes PG (1971) *J Chem Phys* 55:572–579
5. Schleger P, Farago B, Lartigue C, Kollmar A, Richter D (1998) *Phys Rev Lett* 81:124–127
6. Vaca Chávez F, Saalwächter K (2011) *Macromolecules* 44:1549–1559
7. Likhtman AE (2009) *J Non-Newtonian Fluid Mech* 157:158–161
8. Gao J, Weiner JH (1989) *Macromolecules* 22:979–984
9. Krausz AS, Eyring H (1975) *Deformation kinetics*. Wiley, New York
10. Caillard D, Martin JL (2003) *Thermally activated mechanisms in crystal plasticity*, Pergamon Materials Series, vol 8. Elsevier, Lausanne
11. McGrum NG, Buckley CP, Bucknall CB (1997) *Principles of polymer engineering*, 2nd edn. Oxford University Press, New York
12. Kazmierczak T, Galeski A, Argon AS (2005) *Polymer* 46:8926–8936
13. Fetters LJ et al (1994) *Macromolecules* 27:4639–4647
14. Lin YH (1987) *Macromolecules* 20:3080–3083
15. Alefeld GZ (1962) *Naturforsch A* 17:899
16. Martins JA, Zhang W, Brito AM (2006) *Macromolecules* 39:7626–7634
17. Rubinstein M, Colby RH (2003) *Polymer physics*. Oxford University Press, Oxford